Thermochimica Acta 512 (2011) 163–169

Contents lists available at ScienceDirect

Thermochimica Acta

journal homepage: www.elsevier.com/locate/tca

Thermo-chemical characteristics of R134a flow boiling in helically coiled tubes at low mass flux and low pressure

Chang-Nian Chen [a], Ji-Tian Han [a,*], Tien-Chien Jen [b], Li Shao [a]

[a] School of Energy and Power Engineering, Shandong University, No. 17923 Jingshi Rd., Jinan, Shandong Province 250061, PR China
[b] Department of Mechanical Engineering, University of Wisconsin-Milwaukee, Milwaukee, WI 53201, USA

ARTICLE INFO

Article history:
Received 28 June 2010
Received in revised form
24 September 2010
Accepted 30 September 2010
Available online 14 October 2010

Keywords:
Boiling heat transfer
Helically coiled tubes
R134a
Low mass flux and low pressure

ABSTRACT

The characteristics of R134a heat transfer coefficients and wall temperature distribution were investigated under low mass flux and low pressure conditions in a helically coiled tube with heated length of 7070 mm, outer diameter of 10 mm, inner diameter of 7.6 mm, coil diameter of 300 mm and helical pitch of 40 mm. System pressures, mass fluxes and inlet qualities range from 0.20 to 0.75 MPa, 50 to 260 kg/m^2 s and −0.18 to 0.40, respectively. It was found that the wall temperatures in descending segments of coiled tube were higher than those of climbing ones, while the heat transfer coefficients varied inversely. Around the section circumference, the outside temperature was lower than the inside one; this is more apparent at very low mass flux and pressure conditions. The heat transfer coefficient increases with increasing mass flux, vapor quality and heat flux. However, the pressure has an indeterminate effect. New heat transfer coefficient correlations for current conditions were developed comparing with existing correlations.

1. Introduction

Refrigerants from the group of CFCs have a destructive influence on the ozone layer. Global environmental concerns require the use of the environmental-benign refrigerants to replace ozone-depletion refrigerants [1]. Among the alternatives, R134a seems to be similar to R12 in the aspect of thermo-physical properties. However, R134a cannot be directly applied to those systems that use R12 due to the lower thermodynamic efficiency and incompatibility. One alternative way to improve the heat exchanger efficiency with new refrigerant is to redesign the heat exchanger coils of system. The helically coiled tubes, which have a high efficiency in heat transfer rate and compact structure in volume, have been extensively used in engineering applications, including petrochemical, power engineering and chemical engineering, etc. [2–4]. Compared to straight tube, helically coiled tube has higher heat transfer efficiency and compact structure. It has a greater heat transfer area than a straight tube in the same amount of space. This is especially true for applications in aircrafts and submarines, which both need narrow space to operate and the tube should be placed horizontally with a lower gravity center. The advantages of choosing helically coiled tubes over straight tubes make it of practical importance to use helically coiled heat exchangers in heat transfer equipment with R134a as working fluid. Therefore, it is essential that the flow boiling thermo-chemical characteristics of R134a are studied in helically coiled tubes in order to achieve the optimal design and operating performance of the helically coiled heat exchangers.

Since the beginning of last century, laminar and turbulent flow heat transfer in curved or helically coiled tubes has attracted a great interest of researchers due to its enhancement in heat transfer coefficient [5–9]. There were also many experimental investigations performed to study two-phase flow heat transfer in helically coiled heat exchangers, but most of them were conducted using water-vapor flow in vertical helically coiled tubes under medium or high pressure conditions. Owhadi et al. [10] studied heat transfer of water boiling in electrically heated helically coiled pipes and found that the wetting of tube wall at higher qualities was attributed to the secondary flow which forced liquid to the surface closest to helix axis. They developed heat transfer coefficient correlations as functions of Lockhart–Martinelli parameter. Kozeki et al. [11] investigated the heat transfer characteristics of helically coiled tube once-through steam generator. They indicated that the local heat transfer coefficients had little dependence on the system parameters and the locations of coiled tube section. Chen and Zhou [12] observed and explained the mechanism of secondary flow in helically coiled tubes and illustrated the feasibility for correlating experimental data with the Lockhart–Martinelli parameter. Guo et al. [13,14] carried out a series of experimental studies on boiling heat transfer and its instabilities in horizontal helically coiled tubes. It was found that the wall temperature located inner side of one section was higher than that located outer side, and the average heat transfer coefficients in climbing segments were higher than those

* Corresponding author. Tel.: +86 53188399060; fax: +86 53188399060.
E-mail address: jthan@sdu.edu.cn (J.-T. Han).

0040-6031/$ – see front matter © 2010 Elsevier B.V. All rights reserved.
doi:10.1016/j.tca.2010.09.020

Nomenclature

A_e	heated area of the test section (m^2)
B_o	boiling number, $B_o = q_e/G\gamma$
C_p	thermal capacity ($J\,kg^{-1}\,K^{-1}$)
D_c	coil diameter (m)
d_i	inner diameter of the test tube (m)
d_o	outer diameter of the test tube (m)
G	mass flux ($kg\,m^{-2}\,s^{-1}$)
h_l	local heat transfer coefficient ($W\,m^{-2}\,K^{-1}$)
h_{l0}	liquid-phase flow heat transfer coefficient ($W\,m^{-2}\,K^{-1}$)
h_m	average heat transfer coefficient ($W\,m^{-2}\,K^{-1}$)
h_{tp}	two-phase flow heat transfer coefficient ($W\,m^{-2}\,K^{-1}$)
I	current (A)
L	valid heated length (m)
L_l	local tube length from inlet of test section (m)
N_u	Nusselt number, $N_u = h_m d_i/k$
P	pressure (MPa)
Pr	Prandtl number, $Pr = \mu C_P/k$
P_t	helical pitch (m)
Q_e	power supplies for test section (W)
Q_p	power supplies for preheated section (W)
q_e	heat flux of test section ($W\,m^{-2}$)
Re	Reynolds number, $Re = GD/\mu$
s	section symbol of the test tube
T_{lm}	local average inner wall temperature (°C)
T_{sl}	local saturation temperature of the fluid (°C)
T_{sm}	average saturation temperature of the fluid (°C)
T_{wm}	average inner wall temperature of test section (°C)
t	time
U	voltage (V)
X_{tt}	Lockhart–Martinelli parameter
x_i	inlet quality
x_l	local quality

Greek symbols

γ	latent heat of evaporation ($J\,kg^{-1}$)
Δt	subcooled temperature (°C)
η	thermal efficiency
λ	thermal conductivity coefficient ($W\,m^{-1}\,K^{-1}$)
μ	dynamic viscosity (Pa s)
ρ	density ($kg\,m^{-3}$)

Subscripts

g	gas phase
l	liquid phase

in descending segments. For the instabilities in heat transfer, three kinds of oscillation were reported: density wave, pressure drop excursion and thermal fluctuation. In their further work later [15], they investigated the heat transfer and dry-out characteristics in coils with different axis orientations. They divided the boiling flow into three regions: nucleate boiling region, force convection region and post dry-out region, and proposed methods for determining the transition boundary conditions. Zhao et al. [16] conducted a research on heat transfer and pressure drop in a small horizontal helically coiled tubing once-through steam generator. They found that the boiling heat transfer was dependent on both mass flux and heat flux, which implied that it was different from in lager scale tubes where the convection dominated at typical quality regions.

Besides water-vapor flow in helically coiled tubes, there were also many researches available concerning two-phase flow of low latent heat substance (e.g., R134a) in coils. Kang et al. [17] studied the condensation heat transfer and pressure drop of R134a in helically coiled tubes. It was found that the overall condensing heat transfer coefficients of R134a increased with the increase of mass flux, and slowly the pressure drops also increased. They also indicated that helically coiled tube had advantages over straight tube in heat transfer enhancement. Han et al. [18] derived the consistent results with Kang et al. from their experimental investigation under the conditions of different saturated temperatures and found that the saturated temperature had a positive influence on heat transfer coefficients. Wongwises and Polsongkram [19,20] performed evaporation and condensation experiments for R134a two-phase flow heat transfer characteristics in a helically coiled concentric tube-in-tube heat exchanger, respectively. They reported that the heat transfer coefficients in helically coiled heat exchanger were enhanced by 30–37% for evaporation condition and 33–53% for condensation condition, respectively, compared to those in straight tube exchangers. Cui et al. [21] carried out an experimental investigation on R134a two-phase flow heat transfer in both smooth and micro-finned helically coiled tubes. They indicated the same significance of both nucleate boiling and convective boiling in convective boiling in helically coiled tubes, and developed a new heat transfer correlation by introducing Dean number considering the curvature effect of coils. In their further study [22], they conducted the flow pattern and pressure drop experiments in micro-finned helically coiled tubes. Flow patterns and the transition conditions were determined by flow map, and also the pressure drop data were correlated by Lockhart–Martinelli parameter. Lin and Ebadian [23] investigated the condensation heat transfer and pressure drop of R134a in helically coiled concentric tube-in-tube heat exchangers, mainly concerning the effect of the different axis orientations. It was found that the axis orientation had much effect on heat transfer coefficient but less on pressure drop, and the percentage increase of R134a Nusselt number from 0° to 45° was twice than that from 45° to 90° of the axis orientation. In addition, R134a and its mixtures with other refrigerants have been widely used as working fluid for heat transfer investigation [24–28]. Table 1 lists a summary of main literature work related to water or R134a two-phase flow in helically coiled tubes.

An overview of the previous work indicates that few publications concerned the conditions of horizontal axis orientation and the LMLP (low mass flux and low pressure) at the same time for R134a boiling flow in helically coiled tubes. However, the horizontal helically coiled tubes have an extensive application as mentioned above. Also, the LMLP conditions in R134a are very important for fluid modeling of water-vapor, which are equivalent to the medium or high mass flux and pressure conditions in water-vapor. Therefore, the objective of this paper is to experimentally study the R134a boiling flow in a horizontal helically coiled tube at LMLP. The variation of wall temperatures and heat transfer coefficients along the heated length and the circumference of tubes at different positions and the effect of pressure, mass flux, vapor qualities and heat flux on heat transfer coefficients were analyzed and discussed. A new heat transfer coefficient correlation was developed for applications under the present experimental conditions.

2. Experimental system and procedure

2.1. Experimental set-up

The experimental set-up consists of two circle loops: the working loop (R134a) and the cooling loop (30% $CaCl_2$–water), as shown in Fig. 1. It includes the following components: motor pump, Coriolis mass flowmeter, preheated/test sections, precision DC power supplies, condenser, refrigeration chilling unit, N_2-gas accumula-

Table 1
Summary of main literature work related to current investigation.

Author/year	Ranges of parameters	Working fluid	Orientation of coil axis	Boiling/condensation
Owhadi et al./1968 [10]	P = 0.10 MPa; G = 80–315 kg m^{-2} s^{-1}	Water	Vertical	Boiling
Kozeki et al./1970 [11]	P = 0.50–2.1 MPa; G = 161–486 kg m^{-2} s^{-1}	Water	Vertical	Boiling
Chen and Zhou/1986 [12]	P = 0.50–3.5 MPa; G = 200–2400 kg m^{-2} s^{-1}	Water	Vertical	Boiling
Guo et al./1996 [13]	P = 0.5–3.5 MPa; G = 300–1760 kg m^{-2} s^{-1}	Water	Horizontal	Boiling
Bai and Guo/1997 [14]	P = 0.50–3.0 MPa; G = 200–2500 kg m^{-2} s^{-1}	Water	Horizontal	Boiling
Guo et al./1998 [15]	P = 0.40–3.0 MPa; G = 100–2400 kg m^{-2} s^{-1}	Water	Variable	Boiling
Kang et al./2000 [17]	G = 100–420 kg m^{-2} s^{-1}; T = 33 °C	R134a	Vertical	Condensation
Zhao et al./2003 [16]	P = 0.5–3.5 MPa; G = 236–943 kg m^{-2} s^{-1}	Water	Horizontal	Boiling
Han et al./2005 [18]	G = 100–420 kg m^{-2} s^{-1}; T = 35 °C, 40 °C, 46 °C	R134a	Vertical	Condensation
Wongwises and Polsongkram/2006 [19,20]	G = 400–800 kg m^{-2} s^{-1}; T = 10–20 °C	R134a	Vertical	Boiling
	T = 40–50 °C	R134a	Vertical	Condensation
Cui et al./2006 [21]	P = 0.50–0.58 MPa; G = 65–320 kg m^{-2} s^{-1}	R134a	Vertical	Boiling
Lin and Ebadian/2007 [23]	G = 60–200 kg m^{-2} s^{-1}; T = 30 °C, 35 °C	R134a	Variable	Condensation
Cui et al./2008 [22]	P = 0.49–0.58 MPa; G = 70–380 kg m^{-2} s^{-1}	R134a	Vertical	Boiling

tor and data acquisition system. The working loop is designed for pressure of 1.6 MPa and temperature of 200 °C; preheated section power supply of 24 V × 300 A; and test section power supply of 60 V × 500 A. The refrigeration chilling unit has a maximum output of 50 kW.

2.2. Test section and installation

The test section is made of stainless steel tube (SUS304), structure parameter ranges of which are shown in Table 2. The test section was directly heated by high current DC power supplies to generate constant heat flux (ignoring resistance variety of metal material).

The temperatures of the R134a flow at the inlets and outlets of the preheated and test sections are measured with 0.3 mm T-type sheathed thermocouples. And the precision pressure sensors are set at the same positions as thermocouples in order to measure pressures accurately. The temperatures of outside wall are measured by 0.2 mm T-type thermocouples set along the test tube. Eight symmetrical positions of each coil of the helically coiled tube, as s1–s8

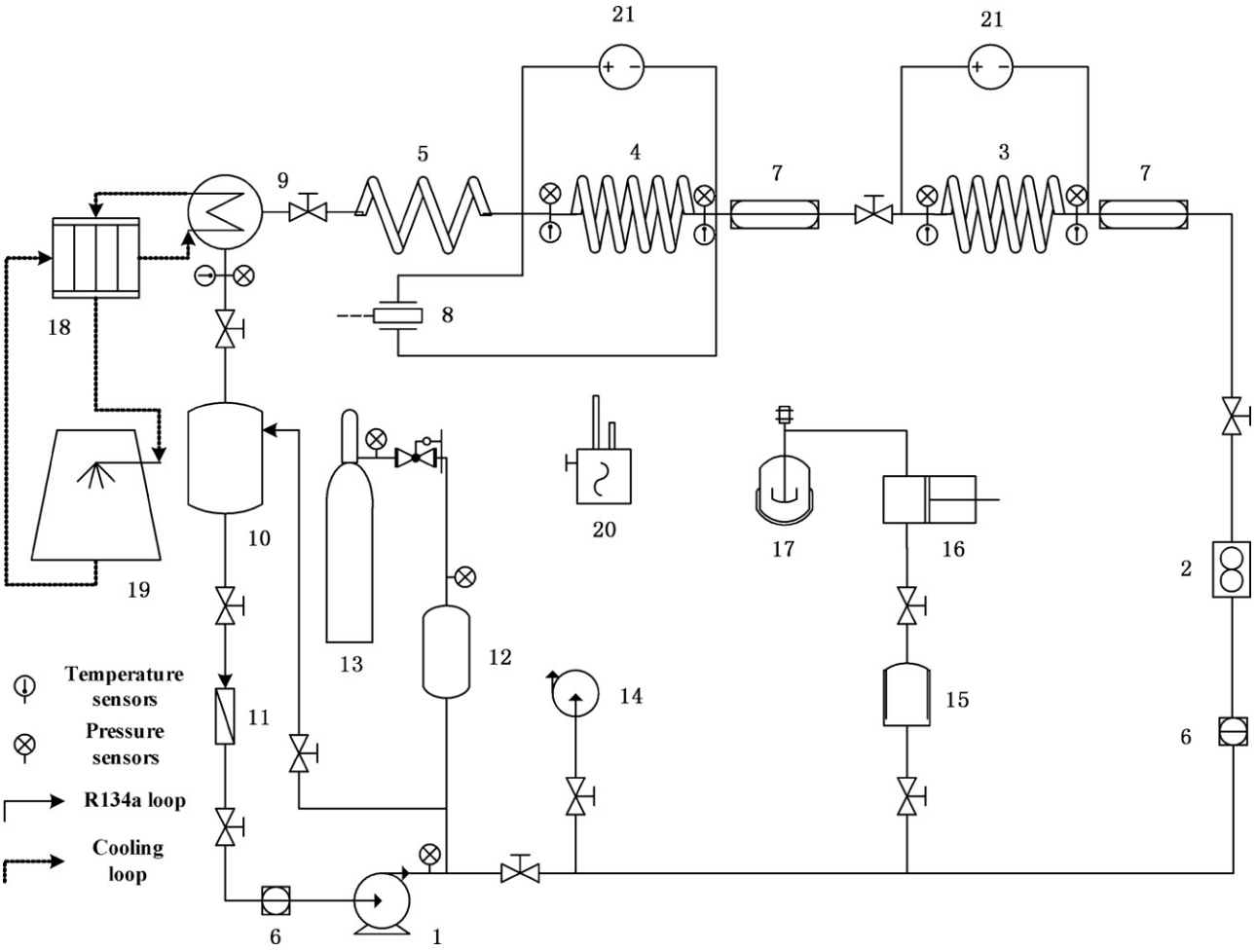

Fig. 1. Schematic diagram of the experimental circle loop. (1) motor pump, (2) Coriolis mass flowmeter, (3) preheated section, (4) test section, (5) flow pattern observing section, (6) sight glass, (7) visual section, (8) differential pressure gage, (9) condenser, (10) receiver tank, (11) dry-strainer, (12) accumulator, (13) N_2 gas tank, (14) vacuum pump, (15) buffer tank, (16) refrigerant pump, (17) refrigerant tank, (18) chilling unit, (19) cooling tower, (20) halogens leak detector and (21) DC power supply.

Table 2
Geometrical parameters of the test section.

Material of tube	Outer diameter, d_o (mm)	Inner diameter, d_i (mm)	Coil diameter, D_c (mm)	Valid heated length, L (mm)	Helical pitch, P_t (mm)
SUS304 stainless steel	10	7.6	300	7070	40

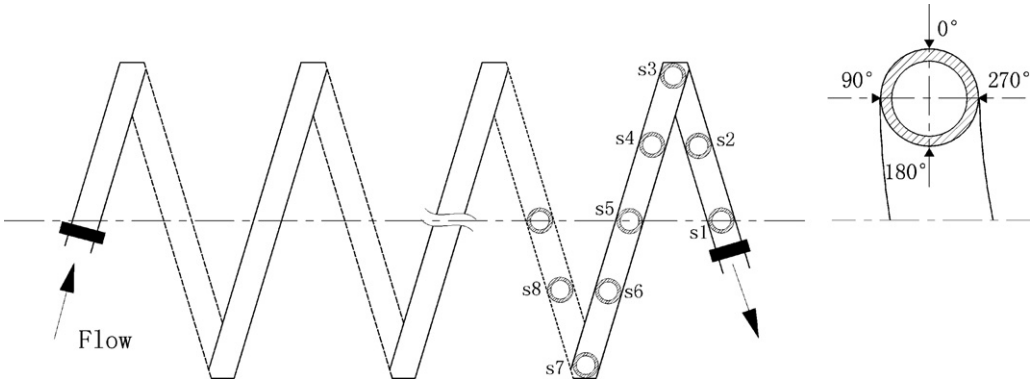

Fig. 2. Schematic diagram of the installation of thermocouples.

Table 3
Experimental condition ranges.

Pressure (MPa)	Mass flux (kg m^{-2} s^{-1})	Inlet quality	Heated power (W)
0.20–0.75	50–260	−0.18–0.40	115–2100

indicated in Fig. 2, are selected as measuring sections where four thermocouples are set evenly around the circumferences, as 0°, 90°, 180° and 270° indicated in Fig. 2. A total of 228 thermocouples are set with 32 in every coil. The test tube was wrapped with 20 mm thick PEF (Polyethylene chemical bridging highly foamed materials) for heat preservation, and metal clamps were installed to stop from distortion of the coiled tube.

2.3. Experimental conditions and procedure

Experimental conditions are listed in Table 3. The helically coiled tube was placed horizontally and connected to the system with flange insulated. Before each single experiment under different conditions, heat balance testing was conducted and the testing results showed that the average heat loss was no more than 5%. The refrigerant R134a is pumped from the receiver tank through a filter-dryer and a mass flow meter to the electrical pre-heater to achieve the set vapor quality at the inlet of the test section. The refrigerant enters the test section and is heated directly by the DC power supply connected to the test section. After leaving the test section, the refrigerant condenses and is collected in the receiver tank. The mass flux can be controlled by adjusting the speed of pump motor and control valves at bypass. The pressure is controlled by adjusting mass flux of cooling loop, power supply of preheated section and N_2-gas accumulator. The heat power is controlled by the precision DC power supplies automatically. All the experimental signals are transmitted to Agilent 34980A data acquisition system for processing.

3. Experimental results and discussion

3.1. Data reduction

The thermo-physical properties of working fluid R134a are obtained from REFPROP Version 8.0 [29]. The heat input from the DC power supply to the test section can be calculated from the measured voltage and current, considering the average heat loss of 5%. Cui et al. [21] employed the same correction for data process to obtain accurate results.

$$Q_e = 0.95U \cdot I \tag{1}$$

The average boiling heat transfer coefficient is defined as:

$$h_m = \frac{q_e}{T_{wm} - T_{sm}} \tag{2}$$

where T_{wm} and T_{sm} are derived from the measured outer wall temperature by considering one-dimensional heat conduction through the wall and the average value of the temperatures at the inlet and outlet, respectively; q_e can be calculated as follows:

$$q_e = \frac{Q_e}{A_e} \tag{3}$$

The local boiling heat transfer coefficient is defined as:

$$h_l = \frac{q_e}{T_{lm} - T_{sl}} \tag{4}$$

$$\frac{d^2t}{dr^2} + \frac{1}{r}\frac{dt}{dr} + \frac{1}{\lambda}\frac{d\lambda}{dt}\left(\frac{dt}{dr}\right)^2 + \frac{Q\eta}{Al\lambda} = 0 \tag{5}$$

where T_{lm} and T_{sl} are derived from the average of the reading of the four thermocouples at the four positions (0–270°) by one-dimensional heat conduction equation through the wall Eq. (5) and a linearly interpolating method of the inlet and outlet temperature of the fluid, respectively.

The local vapor quality for the test section can be calculated by Eqs. (6) and (7).

$$x_i = \frac{4Q_p}{\pi d_i^2 G\gamma} - \frac{C_p\,\Delta t}{\gamma} \tag{6}$$

$$x_l = x_i + \frac{4L_l q_e}{Gd_i\gamma} \tag{7}$$

3.2. Results and discussion

The wall temperature distribution in horizontal helically coiled tubes is shown in Fig. 3(a)–(d). The average wall temperatures of sections decrease along the heated tubes at fixed conditions of pressure and mass flux, as shown in Fig. 3(a). Actually, the variation of temperatures changes very little. Those temperatures in descending sections of coiled tube are higher than those of climbing sections, which may suggest a difference in the heat transfer

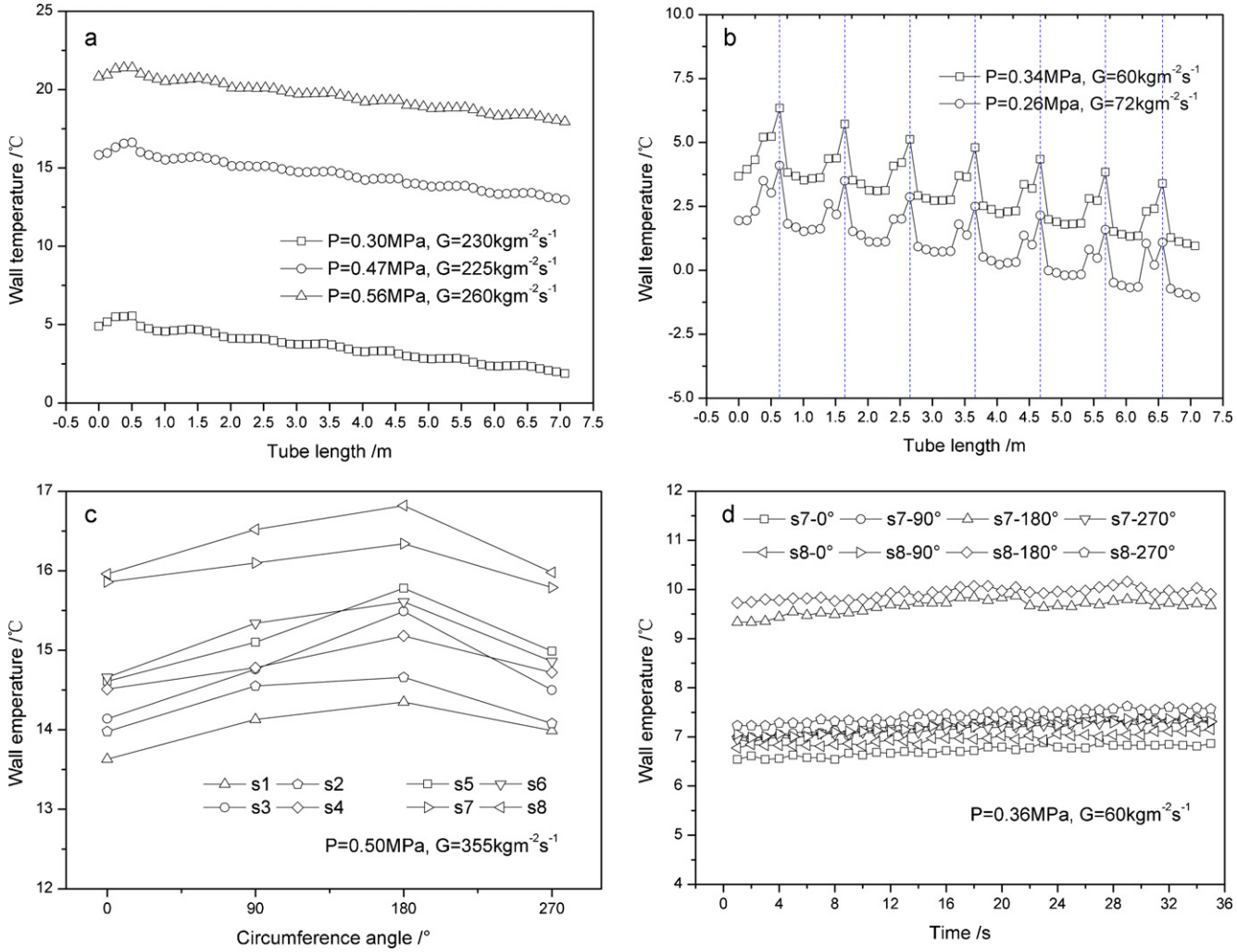

Fig. 3. (a) Characteristics of wall temperature distribution with tube length (general situations). (b) Characteristics of wall temperature distribution with tube length (under very low mass flux and pressure conditions). (c) Characteristics of wall temperature distribution around section circumference (general situations). (d) Characteristics of wall temperature distribution around section circumference (under very low mass flux conditions).

coefficients of the two sections. However, the variation of the temperatures along tube length dramatically changes at very low mass flux and pressure conditions, as shown in Fig. 3(b). It might be caused by the instability of two-phase flow boiling. Guo et al. [13] observed the similar thermal oscillation accompanied by density wave oscillation, which is caused by lower mass flux and relative higher heat flux or wall temperature. The average temperatures at the fourth section of descending section of horizontal helically coiled tube (e.g., s8 indicated in Fig. 2) are usually much higher than other neighboring ones, and a periodic trend is shown in Fig. 3(b). The variation of temperatures at the four positions around one section (0–270°) has been shown in Fig. 3(c) and (d). The temperatures at the undersides (180°) are usually highest, while those at the upsides (0°) are lowest. Those at fronts and offsides (270° and 90°) are intervenient. This situation appears very clearly at lower mass flux. As shown in Fig. 3(d), the temperatures at the undersides are much higher than the others at mass flux of 60 kg/m^2 s and pressure of 0.36 MPa.

The average boiling heat transfer coefficients as a function of R134a mass flux at different pressures for the horizontal helically coiled section are shown in Fig. 4(a). It can be seen that the average boiling heat transfer coefficients increase approximate linearly with increasing the mass flux of R134a. Fig. 4(b) illustrates the variation of the local boiling heat transfer coefficient with the vapor quality at different mass fluxes of R134a. The results show that the local heat transfer coefficients increase with increasing the vapor qualities; the mass flux has a strong effect on the local boiling heat transfer coefficients, especially at high qualities. This may be explained that not only the interfacial gas–liquid shear stress and the degree of turbulence of the fluid, but also the intensity of the secondary flow are increased with the high velocity due to increase of mass flux. The effect of heat flux on the local boiling heat transfer coefficients at different vapor qualities is shown in Fig. 4(c). It can be noted that the local heat transfer coefficients monotonously increased with the vapor quality at low heat flux. When the heat fluxes increase to a higher level, the heat transfer coefficients reach maximum at a vapor quality of about 0.70, then decrease slightly with the vapor quality. The similar result was obtained by Boissieux et al. [30] but for a straight tube. At LMLP conditions, the effect of the pressure is more complex. In general, at relative high mass flux heat transfer coefficients minutely increase with the increasing of pressure, as indicated in Fig. 4(a), but at very low mass flux, it has an indeterminate effect. Furthermore, the pressure has the least significant effect among all the above system parameters under the present conditions.

3.3. Comparison with prediction results

For the purpose of correlating experimental data, the Lockhart–Martinelli parameter method [11,14,31,32] is feasible

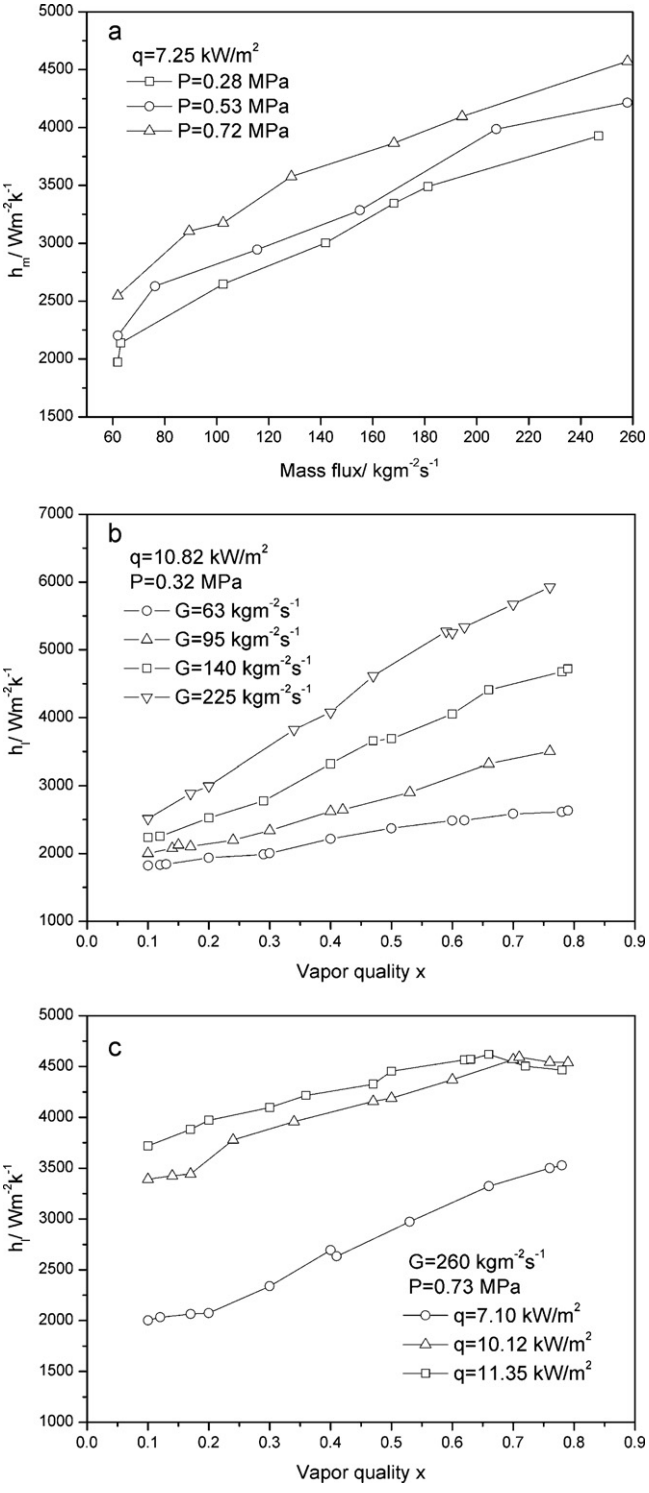

Fig. 4. (a) Average boiling heat transfer coefficients vs mass flux. (b) Local heat transfer coefficients vs vapor quality at different mass fluxes. (c) Local heat transfer coefficients vs vapor quality at different heat fluxes.

and easily to use for heat transfer coefficient correlations. It is expressed as:

$$\frac{h_{tp}}{h_{l0}} = c_1\left(\frac{1}{X_{tt}}\right)^{c_2} \tag{8}$$

where c_1 and c_2 are derived from experimental data, respectively.

Kozeki [11] and Bai [14] correlations are based on the Lockhart–Martinelli parameter method, the specific expressions of

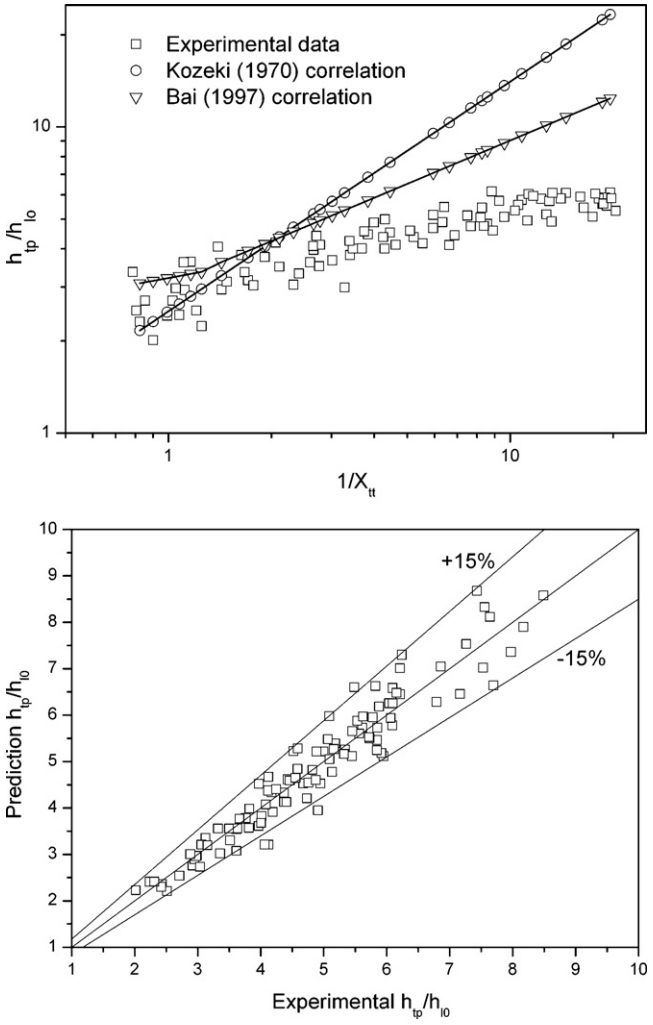

Fig. 5. (a) Comparison of experimental data with Bai [14] and Kozeki [11] correlations. (b) Comparison of experimental data with new correlation.

which are given in Eqs. (9) and (10). Current experimental data were compared with Kozeki and Bai correlations at the same conditions, as shown in Fig. 5(a). It shows that the calculated values from Kozeki correlation are more dispersed than the experimental data. Though Bai's correlation has a better result, most of the predicted data are higher than experimental ones.

$$\frac{h_{tp}}{h_{l0}} = 2.5\left(\frac{1}{X_{tt}}\right)^{0.75} \tag{9}$$

$$\left.\begin{aligned}\frac{h_{tp}}{h_{l0}} &= 1 + 2.21\left(\frac{1}{X_{tt}}\right)^{0.3}, \quad \frac{1}{X_{tt}} < 1.2\\ \frac{h_{tp}}{h_{l0}} &= 3.06\left(\frac{1}{X_{tt}}\right)^{0.47}, \quad \frac{1}{X_{tt}} \geq 1.2\end{aligned}\right\} \tag{10}$$

A new heat transfer coefficient correlation for current experimental conditions was developed based on the Lockhart–Martinelli parameter method with an error of ±15%, as indicated in Fig. 5(b).

$$\left.\begin{aligned}\frac{h_{tp}}{h_{l0}} &= 2.84\left(\frac{1}{X_{tt}}\right)^{0.27} + (46162B_o^{1.15} - 0.88)\\ X_{tt} &= \left(\frac{1-x}{x}\right)^{0.9}\left(\frac{\rho_g}{\rho_l}\right)^{0.5}\left(\frac{\mu_l}{\mu_g}\right)^{0.1}\end{aligned}\right\} \tag{11}$$

where h_{tp} and h_{l0} can be derived from experimental data and single-phase heat transfer correlations Eq. (12) proposed by Seban [8],

respectively.

$$\left.\begin{aligned} N_u &= 0.023\, Re^{0.85}\, \mathrm{Pr}^{0.4}\left(d_i/D_c\right)^{0.1} \\ h_{l0} &= \frac{N_u \lambda}{d_i} \end{aligned}\right\} \quad (12)$$

4. Experimental uncertainties

The directly measured parameters in experiments include length, temperature, pressure, mass flux, voltage and current. Based on the instructions from experimental equipment and verified data sheet, the maximum uncertainties in measuring length and inner diameter of test section are ±0.014% and ±0.27%, respectively; the maximum uncertainty in measuring temperature is ±3.6%; the maximum uncertainty in measuring pressure is ±2%; the maximum uncertainty in measuring mass flux is ±2.1%; the maximum uncertainties in measuring voltage and current are ±2% and ±3.8%, respectively. The uncertainty analysis results indicate that the maximum uncertainties in measuring the average and local heat transfer coefficients are ±8.5% and ±11.3%, respectively, according to Moffat's experimental error transfer procedure [33].

5. Conclusions

Characteristics of R134a flow boiling heat transfer in a horizontal helically coiled tube were investigated under low mass flux and low pressure conditions. From the analysis of wall temperature distribution and the boiling heat transfer coefficient, conclusions can be drawn as follows.

(1) Under very low mass flux and pressure conditions, the average wall temperatures of sections decrease along the heated coiled tube at fixed conditions of pressure and mass flux, and the variation of the temperatures greatly changes owing to the instability of two phase flow boiling.
(2) The average temperatures at the fourth section of descending sections of horizontal helically coiled tube are usually much higher than other sections. Around the circumference, the temperatures at the undersides (180°) are usually highest, while those at the upsides (0°) are lowest. Those at fronts and offsides (270° and 90°) are intervenient. It is more apparent with very low mass flux.
(3) In general, the heat transfer coefficients increase with increasing mass flux, heat flux, vapor quality and pressure. Mass flux has much effect on heat transfer coefficients, while pressure has little.
(4) A new heat transfer coefficient correlation for present experimental conditions was developed for applications based on Lockhart–Martinelli parameter with an error of ±15%.

Acknowledgements

This work was supported by The National Natural Science Foundation of China (No.50776055 and No. 51076084). Dr. Tien-Chien Jen would also like to acknowledge partial financial support from EPA (USA) award RD 833357.

References

[1] M.J. Molina, F.S. Rowland, Stratospheric sink of chloromethanes, chlorine atom catalyzed destruction of ozone, Nature 249 (1974) 810–812.
[2] L.J. Guo, Z.P. Feng, X.J. Chen, An experimental investigation of the frictional pressure drop of steam-water two-phase flow in helical coils, Int. J. Heat Mass Transf. 44 (2001) 2601–2610.
[3] R.C. Xin, A. Awwad, Z.F. Dong, M.A. Ebadian, An experimental study of single-phase and two-phase flow pressure drop in annular helicoidal pipes, Int. J. Heat Mass Transf. 18 (1997) 482–488.
[4] B. Yu, J.T. Han, H.J. Kang, C.X. Lin, A. Awwad, M.A. Ebadian, Condensation heat transfer of R-134a flow inside helical pipes at different orientations, Int. Commun. Heat Mass Transf. 30 (2003) 745–754.
[5] G.S. Williams, C.W. Hubbell, G.H. Fenkell, Experiments at Detroit, Mich., on the effect of curvature upon the flow of water in pipes, Trans. ASCE 47 (1902) 1–309.
[6] J. Eustice, Flow of water in curved pipes, Proc. R. Soc. Ser. A 84 (1910) 107–118.
[7] W.R. Dean, The stream-line motion of fluid in a curved pipe, Philos. Mag. J. Sci. 5 (1928) 673–695.
[8] R.A. Seban, E.F. Mclaughlin, Heat transfer in tube coils with laminar and turbulent flow, Int. J. Heat Mass Transf. 6 (1963) 387–395.
[9] Y. Mori, W. Nakayama, Study on forced convective heat transfer in curved pipes (2rd Report, Turbulent Region), Int. J. Heat Mass Transf. 10 (1967) 37–59.
[10] A. Owhadi, K.J. Bell, B. Crain Jr., Forced convection boiling inside helically coiled tubes, Int. J. Heat Mass Transf. 11 (1968) 1779–1793.
[11] M. Kozeki, H. Nariai, T. Furukawa, K. Kurosu, A study of helically coiled tube once-through steam generator, Bull. Jpn. Soc. Mech. Eng. 13 (1970) 1485–1494.
[12] X.J. Chen, F.D. Zhou, Forced convective boiling and post-dryout heat transfer in helical coiled tubes, in: Proceeding of 8th International Heat Transfer Conference, San Francisco, USA, 1986.
[13] L.J. Guo, Z.P. Feng, X.J. Chen, Experimental investigation of forced convective boiling flow instabilities in horizontal helically coiled tubes, J. Therm. Sci. 5 (1996) 210–216.
[14] B.F. Bai, L.J. Guo, Study on convective boiling heat transfer in horizontal helically coiled tubes, Chin. J. Nucl. Sci. Eng. 17 (1997) 302–308.
[15] L.J. Guo, X.M. Zhang, Z.P. Feng, X.J. Chen, Forced convection boiling heat transfer and dry-out characteristics in helical coiled tubes with various axial angles, J. Basic Sci. Eng. 6 (1998) 383–391.
[16] L. Zhao, L.J. Guo, B.F. Bai, Y.C. Hou, X.M. Zhang, Convective boiling heat transfer and two-phase flow characteristics inside a small horizontal helically coiled tubing once-through steam generator, Int. J. Heat Mass Transf. 46 (2003) 4779–4788.
[17] H.J. Kang, C.X. Lin, M.A. Ebadian, Condensation of R134a flowing inside helicoidal pipe, Int. J. Heat Mass Transf. 43 (2000) 2553–2564.
[18] J.T. Han, C.X. Lin, M.A. Ebadian, Condensation heat transfer and pressure drop characteristics of R-134a in an annular helical pipe, Int. Commun. Heat Mass Transf. 32 (2005) 1307–1316.
[19] S. Wongwises, M. Polsongkram, Evaporation heat transfer and pressure drop of HFC-134a in a helically coiled concentric tube-in-tube heat exchanger, Int. J. Heat Mass Transf. 49 (2006) 658–670.
[20] S. Wongwises, M. Polsongkram, Condensation heat transfer and pressure drop of HFC-134a in helically coiled concentric tube-in-tube heat exchanger, Int. J. Heat Mass Transf. 49 (2006) 4386–4398.
[21] W.Z. Cui, L.J. Li, M.D. Xin, T.C. Jen, Q.H. Chen, Q. Liao, A heat transfer correlation of flow boiling in micro-finned helically coiled tube, Int. J. Heat Mass Transf. 49 (2006) 2851–2858.
[22] W.Z. Cui, L.J. Li, M.D. Xin, T.C. Jen, Q. Liao, Q.H. Chen, An experimental study of flow pattern and pressure drop for flow boiling inside microfinned helically coiled tube, Int. J. Heat Mass Transf. 51 (2008) 169–175.
[23] C.X. Lin, M.A. Ebadian, Condensation heat transfer and pressure drop of R134a in annular helicoidal pipe at different orientations, Int. J. Heat Mass Transf. 50 (2007) 4256–4264.
[24] S.J. Eckels, M. Pate, Evaporation and condensation of R134a and CFC-12 in a smooth tube and a micro-fin tube, ASHRAE Trans. 97 (1991) 71–81.
[25] X. Liu, Condensing and evaporating heat transfer and pressure drop characteristics of HFC-134a and HCFC-22, J. Heat Transf. 119 (1997) 158–163.
[26] T.Y. Choi, T.J. Kim, M.S. Kim, S.T. Ro, Evaporation heat transfer of R-32, R-134a, and R-32/125/134a inside a horizontal smooth tube, Int. J. Heat Mass Transf. 43 (2000) 3651–3660.
[27] D. Jung, Y. Cho, K. Park, Flow condensation heat transfer coefficients of R22, R134a, R407C, and R410A inside plain and micro-fin tubes, Int. J. Refrig. 27 (2004) 25–32.
[28] J.R. Thome, Update on advances in flow pattern based two-phase heat transfer models, Exp. Therm. Fluid Sci. 29 (2005) 341–349.
[29] NIST, REFPROP, Version 8.0, US Department of Commerce, USA, 2007.
[30] X. Boissieux, M.R. Heikal, R.A. Johns, Two-phase heat transfer coefficients of three HFC refrigerants inside a horizontal smooth tube. Part 1: evaporation, Int. J. Refrig. 23 (2000) 269–283.
[31] R.C. Martinelli, D.B. Nelson, Prediction of pressure drop during forced circulation of water, J. Heat Transf. 70 (1948) 659–702.
[32] R.W. Lockhart, R.C. Martinelli, Proposed correlations for isothermal two-phase, two-component flow in pipes, Chem. Eng. Process. 45 (1949) 39–48.
[33] R.J. Moffat, Describing the uncertainties in experimental results, Exp. Therm. Fluid Sci. 1 (1988) 3–17.